

The effects of injection beam parameters and foil scattering for CSNS/RCS^{*}

Huang Ming-Yang¹⁾ Wang Sheng Qiu Jing Wang Na Xu Shouyan

(Institute of High Energy Physics, Chinese Academy of Sciences, Beijing 100049, China)

Abstract The China Spallation Neutron Source (CSNS) uses H^- stripping and phase space painting method to fill large ring acceptance with the linac beam of small emittance. The dependence of the painting beam on the injection beam parameters was studied for the Rapid Cycling Synchrotron (RCS) of CSNS. The injection processes for different momentum spread, rms emittance of the injection beam, injection beam matching were simulated, then the beam losses, 99% and rms emittances were obtained and the optimized ranges of injection beam parameters were given. The interaction between the H^- beam and the stripping foil was studied and the foil scattering was simulated. Then, the stripping efficiency was calculated and the suitable thickness of the stripping foil was obtained. The energy deposition on the foil and the beam losses due to the foil scattering were also studied.

Key words CSNS; RCS; Injection parameter; Foil scattering

PACS 29.25.Dz, 29.27.Ac, 41.85.Ar, 34.50.Fa

1 Introduction

CSNS is a high power proton accelerator-based facility^[1]. The accelerator consists of a 1.6GeV RCS and an 80MeV H^- linac which is upgradable to 250MeV. The RCS accumulates 1.56×10^{13} protons in two intense bunches and operates at a 25Hz repetition rate with a design beam power of 100kW, and is capable of upgrading to 500kW. It has a four-fold lattice with four long straight sections for the injection, extraction, RF and beam collimation.

For high intensity proton accelerators, injection via H^- tripping is a practical method. The design of the RCS injection system is to inject the H^- beam into the RCS with high precision and high transport efficiency. In order to control the strong space charge effects which are the main causes of the beam losses in CSNS/RCS, the phase space painting method is used for injecting the beam of small emittance from the linac into the large ring acceptance^[2]. With the code ORBIT^[3], the multi-turn phase space painting injection process with space charge effects for CSNS/RCS is studied in detail.

When the H^- beam traverses the stripping foil, most of the particles H^- are converted to H^+ , and the others are converted to H^0 or unchanged. The in-

teraction with the stripping foil can induce the beam emittance growth and beam loss. With the code FLUKA^[4], the foil scattering due to the interaction between the H^- beam and the stripping foil is simulated, and the stripping efficiency is calculated. The energy deposition on the foil and the beam losses due to the foil scattering are also studied.

2 Dependence of the painting beam on the injection beam parameters

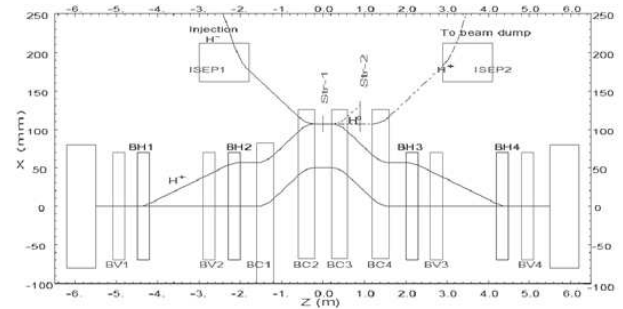


Fig. 1. Layout of the RCS injection system.

For CSNS, combination of the H^- stripping and phase space painting method are used to accumulate high intensity beam in the RCS. Fig. 1 shows

^{*} supported by National Natural Science Foundation of China (Project Nos. 11175020 and 11175193)

¹⁾ E-mail: huangmy@ihep.ac.cn

the layout of the RCS injection system^[2] and Table 1 shows the main injection parameters^[5]. For the beam injection, three kind of orbit-bump systems are prepared^[2]. One is a horizontal bump system (four dipole magnets; BH1-BH4) for painting in $x-x'$ plane; one is a vertical bump system (four dipole magnets; BV1-BV4) for painting in $y-y'$ plane; the third one is a horizontal bump system (four dipole magnets; BC1-BC4) in the middle for an additional closed-orbit shift of 47mm.

Table 1. Main injection parameters of CSNS/RCS.

Parameters/units	Values
Circumference/m	227.92
Injection energy/GeV	0.08
Extraction energy/GeV	1.6
Injection beam power/kW	5
Extraction beam power/kW	100
Nominal betatron tunes	4.86/4.78
RF frequency/MHz	1.0241 ~ 2.3723
RF voltage/kV	165
Harmonic number	2
Repetition rate/Hz	25
Number of particles per pulse	1.56×10^{13}
Momentum acceptance	1%
Painting scheme	Anti-Correlated
Chopping rate	50%
Turn number of injection	200

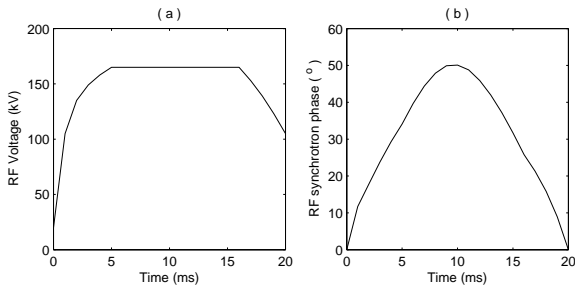


Fig. 2. The patterns of the RF voltage and synchronous phase over the acceleration period.

In the RCS, the emittance evolution and beam losses depend on the injection beam parameters, such as the injection emittance, starting injection time, injection beam matching, momentum spread, and chopping rate. Some works have been done for the injection parameters optimization^{[6][7]}. In this section, the effects of the momentum spread, the *rms* emittance of the injection beam, and the injection twiss parameters mismatch are discussed in detail. In the falling simulation, the chopping rate is 50%, the patterns of

the RF voltage and synchrotron phase are given in Fig. 2, and the space charge effects are considered. At the same time, the turn number of the injection painting process is 200 and only 2000 turns in the acceleration process are considered for the simulation.

2.1 Momentum spread

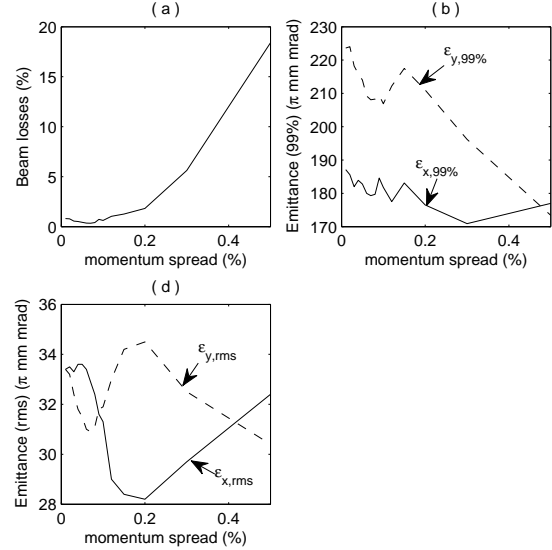


Fig. 3. Beam losses, 99% and *rms* emittances as a function of the momentum spread.

The code ORBIT is used for the injection simulation, it can perform the painting injection process and include the space charge effects. By using ORBIT, the injection processes with the momentum spread between 0.01% and 0.5% were simulated. Fig. 3 shows the beam losses, 99% and *rms* emittances as a function of the momentum spread and Fig. 4 shows the *rms* emittance evolution for different momentum spread. It can be found from Fig. 3 that the beam losses decrease firstly and then increase with the increasing momentum spread. While the momentum spread smaller than 0.1%, the beam losses are smaller than 1%, the 99% and *rms* emittances are constrained in reasonable ranges.

It can be found from Fig. 4 that there is transverse coupling between x and y *rms* emittance evolutions which depends on the momentum spread. When the momentum spread is below 0.1%, the coupling becomes stronger and stronger with the increasing momentum spread. However, when the momentum spread is above 0.1%, the coupling becomes weaker and weaker with the increasing momentum spread. Therefore, the momentum spread of 0.1% is a optimal value for the injection. This simulation results

are consistent with the running experiments in J-PARC^[8].

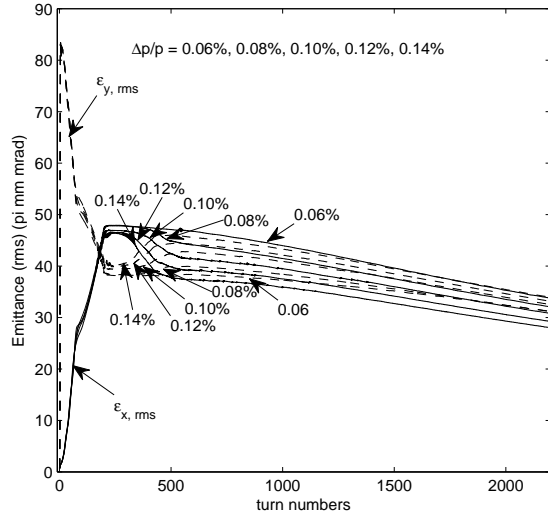


Fig. 4. The *rms* emittance evolution for different momentum spreads.

2.2 *rms* emittance of the injection beam

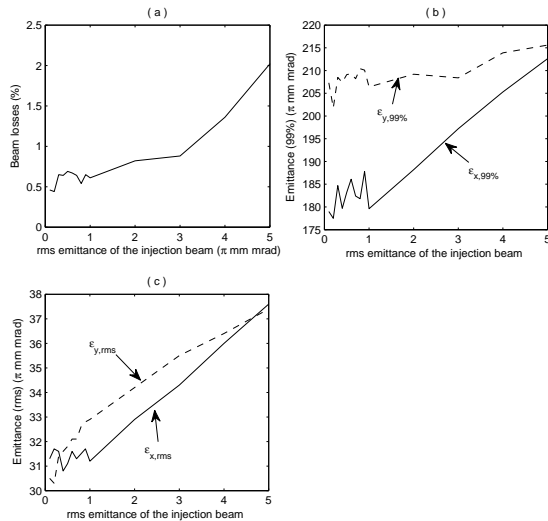


Fig. 5. Beam losses, 99% and *rms* emittances as a function of the *rms* emittance of the injection beam.

In order to study the effects of the *rms* emittance of the injection beam, the injection processes with the *rms* emittance between $0.1\pi\text{mm}\cdot\text{mrad}$ and $5.0\pi\text{mm}\cdot\text{mrad}$ were simulated. Fig. 5 shows the beam losses, 99% and *rms* emittances as a function of the *rms* emittance of the injection beam. It can be

found that the beam losses, 99% and *rms* emittances all increase with the increasing *rms* emittance of the injection beam. In addition, while the *rms* emittance of the injection beam is smaller than $1.0\pi\text{mm}\cdot\text{mrad}$, the beam losses are smaller than 1%, the 99% and *rms* emittances are constrained in reasonable ranges.

2.3 Injection twiss parameters mismatch

For the RCS design, it has been a primary concern to match the physical parameters of the linac and the RCS at the injection point. A mismatched injection could result in large beam losses and an undesirable transverse emittance growth. The first condition for the injection beam matching is obtained by choosing the parameters^[9]:

$$\frac{\alpha_l}{\beta_l} = \frac{\alpha_r}{\beta_r}, \quad (1)$$

where α_l and β_l are the twiss parameters for the linac and α_r and β_r for the RCS. For CSNS, α_r nearly equals to 0. In order to study the effects of the injection twiss parameters mismatch, for a fixed β_l , the injection processes for different α_l were discussed.

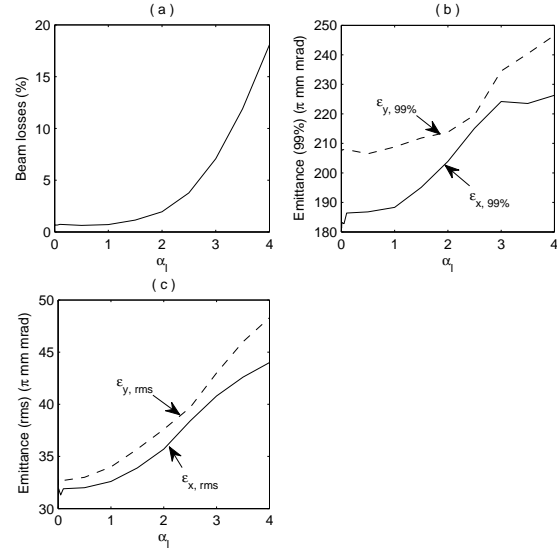


Fig. 6. Beam losses, 99% and *rms* emittances as a function of α_l .

The injection processes with $(\alpha_{lx}, \alpha_{ly})$ between $(0.0, 0.0)$ and $(5.0, 5.0)$ were simulated. Fig. 6 shows the beam losses, 99% and *rms* emittances as a function of α_l . It can be found that the beam losses, 99% and *rms* emittances all increase with the increasing α_l . While $(\alpha_{lx}, \alpha_{ly})$ smaller than $(1.0, 1.0)$, the beam losses are smaller than 1%, the 99% and *rms* emittances are constrained in reasonable ranges, i.e. the effects of the injection twiss parameters mismatch are very small. However, while $(\alpha_{lx}, \alpha_{ly})$ larger than $(1.0,$

1.0), the beam losses, 99% and *rms* emittances are much larger than that of the match case, i.e. the injection beam should not be matched into the RCS acceptance.

In the above discussions, we have studied the effects of the momentum spread, the *rms* emittance of the injection beam, and the injection twiss parameters mismatch. It can be found that the beam losses are smaller than 1%, the 99% and *rms* emittances are constrained in reasonable ranges while the momentum spread smaller than 0.1%, the *rms* emittances of the injection beam smaller than $1.0\pi\text{mm}\cdot\text{mrad}$, and $(\alpha_{lx}, \alpha_{ly})$ smaller than (1.0, 1.0). The momentum spread of 0.1% is a optimal value for the injection, and the injection beam should be well matched into the RCS acceptance when $(\alpha_{lx}, \alpha_{ly})$ smaller than (1.0, 1.0).

3 Foil scattering effects

In the injection system of the RCS, there are two carbon stripping foils, a primary stripping foil and a secondary stripping foil. In this section, the interaction between the H^- beam and the primary stripping foil is discussed^{[10][11][12]} and the stripping efficiency is calculated. The energy deposition on the foil and the beam losses due to the foil scattering are also studied.

3.1 Foil stripping

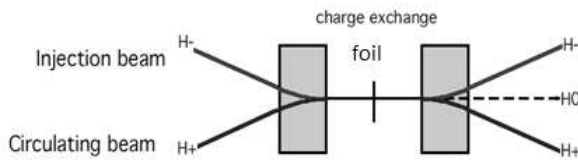


Fig. 7. The production of H^- , H^0 , H^+ by foil stripping.

When the H^- beam traverses the carbon stripping foil^[13], there are six charge exchange processes: three are electron loss reactions and three are electron pickup reactions. However, for energies above 100keV, the cross sections for electron pickup are very small and can be neglected. Therefore, the remain particles after foil stripping are H^- , H^0 and H^+ , as shown in Fig. 7. The stripping efficiency of H^+ is given by^[14]

$$f_{H^+} = 1 - \frac{1}{\sigma_{-1,0} + \sigma_{-1,1} - \sigma_{0,1}} \left[\sigma_{-1,0} e^{-\sigma_{0,1}x} - (\sigma_{0,1} - \sigma_{-1,1}) e^{-(\sigma_{-1,0} + \sigma_{-1,1})x} \right], \quad (2)$$

where $\sigma_{-1,0}$, $\sigma_{0,1}$, $\sigma_{-1,1}$ are the cross-sections of the reactions $H^- \rightarrow H^0 + e^-$, $H^0 \rightarrow H^+ + e^-$, and $H^- \rightarrow H^+ + e^- + e^-$, respectively. In addition, $x = N_o \tau / A$, where N_o is the Avogadro's constant, A is the atomic number of the carbon foil, and τ is the area density. The percent of the H^- beam traverses the carbon foil without stripping is given by^[14]

$$f_{H^-} = e^{-\sigma_{-1,0}x}. \quad (3)$$

Therefore, the yielding rate of H^0 can be expressed as

$$f_{H^0} = 1 - f_{H^+} - f_{H^-}. \quad (4)$$

There are some studies^{[14][15]} about the cross-sections $\sigma_{-1,0}$, $\sigma_{0,1}$, $\sigma_{-1,1}$ which depend on the beam energy. Table 2 shows a summary of the cross-sections at 80MeV and 250MeV.

Table 2. Cross-sections of H^- incident on carbon foil (unit 10^{-18}cm^2).

	80MeV	250MeV
$\sigma_{-1,0}$	3.17	1.35
$\sigma_{0,1}$	1.24	0.53
$\sigma_{-1,1}$	0.056	0.024

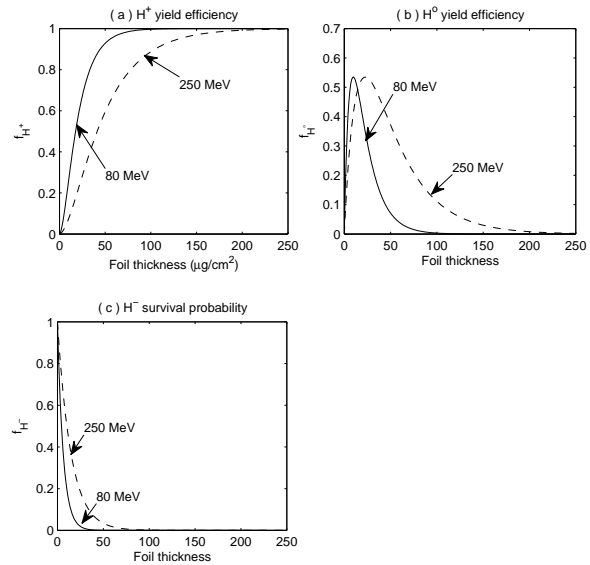


Fig. 8. H^- , H^0 , H^+ yielding rates as a function of the foil thickness.

Using Eqs. (2)- (4) and the cross-sections given in Table 2, the relations between f_{H^+} , f_{H^0} , f_{H^-} and the foil thickness can be obtained. Fig. 8 shows the curves that f_{H^+} , f_{H^0} , f_{H^-} vary with the foil thickness. It can be found that, with the increasing thickness of the foil, f_{H^+} increases, f_{H^-} decreases, and

f_{H^0} has a maximum value. For a given foil thickness, the stripping efficiency for 80MeV injection is larger than that for 250MeV injection. For CSNS/RCS injection system, in order to make the stripping efficiency greater than 99.7%, the thickness of the stripping foil need to be larger than $100\mu\text{g}/\text{cm}^2$ for 80MeV injection and $240\mu\text{g}/\text{cm}^2$ for 250MeV injection.

3.2 Energy deposition on the foil

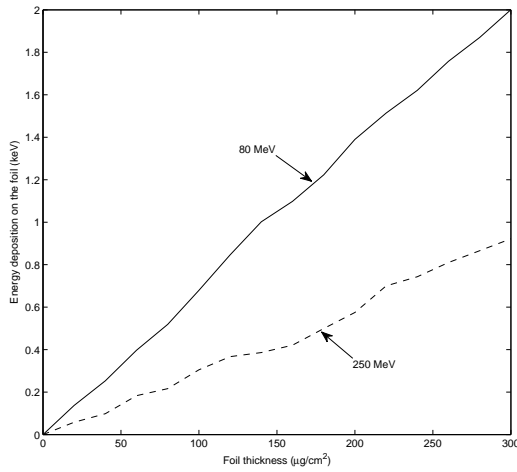


Fig. 9. The energy deposition as a function of the foil thickness.

When the H^+ beam traverses the stripping foil, there is an energy deposition on the foil due to the foil scattering. The energy deposition depends on the beam energy and the foil thickness^[12]. In this part, the relations between the energy deposition and the thickness of the stripping foil for different injection energy are studied.

By using the code FLUKA, the foil scattering process were simulated when the H^+ beam traverses the stripping foil. Fig. 9 shows the energy deposition on the foil as a function of the thickness of the stripping foil. Both for 80MeV injection and 250MeV injection, it can be found that the energy deposition increases with the increasing thickness of the stripping foil. In addition, the relations between the energy deposition and the foil thickness are nearly linear. Furthermore, the energy deposition on the foil is 0.68keV for 80MeV injection ($100\mu\text{g}/\text{cm}^2$) and 0.74keV for 250MeV injection ($240\mu\text{g}/\text{cm}^2$).

3.3 Beam losses

During the injection process, the foil scattering will generate the beam halo and result in additional

beam losses. For J-PARC, the stripping foil scattering has been studied and it can be found that the foil scattering is the main cause of beam losses in the injection region^[16]. Therefore, the beam losses due to the foil scattering for CSNS/RCS also need to be studied in detail. By using the codes FLUKA and ORBIT, the injection process and foil scattering can be simulated. Table 3 shows the beam parameters for 80MeV injection and 250MeV injection.

Table 3. Beam parameters for 80MeV injection and 250MeV injection.

Injection	80MeV	250MeV
Injection beam power/KW	5	80
Average injection current/ μA	62.5	312.5
Turn number of injection	200	403
Foil thickness/ $(\mu\text{g}/\text{cm}^2)$	100	240

By using the code ORBIT, the injection process can be simulated, the average traversal number and the beam distribution after injection can be obtained. Calculating those particles of the beam distribution which are in the range of the stripping foil, the twiss parameters and 99% emittance for those particles can be obtained, as shown in Table 4. With these beam parameters, the beam distribution that hitting on the stripping foil can be simulated. Then, the foil scattering process can be simulated by the code FLUKA and the beam losses due to the foil scattering in single turn can be obtained. By using the average traversal number, the foil scattering induced beam losses during the multi-turn injection process can be calculated. Table 5 shows a summary of the beam losses due to the foil scattering. It can be found that the beam losses are about 0.3W for 80MeV injection and 4.6W for 250MeV injection.

Table 4. Beam parameters of the proton distribution that hitting on the stripping foil.

Injection	80MeV	250MeV
(α_x, α_y)	(0.003, 0.044)	(0.001, 0.016)
$(\beta_x, \beta_y)/\text{m}$	(1.833, 4.458)	(1.877, 5.222)
$(\gamma_x, \gamma_y)/\text{m}^{-1}$	(0.546, 0.225)	(0.533, 0.192)
$(\varepsilon_{x,99\%}, \varepsilon_{y,99\%})/(\pi \cdot \text{mm} \cdot \text{mrad})$	(92, 247)	(90, 282)

Table 5. Beam losses due to the stripping foil scattering.

Injection	80MeV	250MeV
Average traversal number	5	10
Particle loss ratio in single turn	0.0012%	0.00058%
Total beam losses/W	0.3	4.6

4 Conclusions

The dependence of the painting beam on the injection beam parameters for CSNS/RCS were studied and the injection processes for different momentum spread, *rms* emittance of the injection beam, and injection beam matching had been discussed. The beam losses, 99% and *rms* emittances were obtained, and the optimized ranges of injection beam param-

eters were given. The interaction between the H^- beam and the stripping foil was studied. Then, the stripping efficiency of H^+ and the yielding rates of H^- and H^0 were calculated. The energy deposition on the foil and the beam losses due to the foil scattering were also studied.

The authors would like to thank CSNS colleagues for the discussions and consultations.

References

- 1 Wang S, Fang S X, Fu S N et al. Chin. Phys. C, 2009, **33**: 1-3
- 2 Tang J Y, Qiu J, Wang S et al. Chin. Phys. C, 2006, **30**: 1184-1189
- 3 Gabambos J, Holmes J, Olsen D, ORBIT User's Manual V1.0, SNS-ORNL-AP Tech. Note 11, 1999.
- 4 Ferrari A, Fasso A, Ranft J et al. Fluka: multi-particle transport code, CERN-2005-010, 2008.
- 5 CSNS Project Team. China Spallation Neutron Source Feasibility Reaearch Report. Institute of High Energy Physics and Institute of Physics, Chinese Academy of Sciences, 2009 (in Chinese)
- 6 Qiu J, Tang J Y, Wang S et al. Chin. Phys. C, 2007, **31**: 942-946
- 7 Wei T, Wang S, Qiu J et al. Chin. Phys. C, 2010, **34**: 218-223
- 8 Wei G H, Beam injection and fast extraction tuning of the J-PARC MR, and some study on the J-PARC Linac, IHEP Report, January 2012
- 9 Beebe-Wang J and Prior C R, Injection mismatch for the SNS accumulator ring, BNL/SNS TECHNICAL NOTE, NO. 086, June 1, 2000
- 10 Mohagheghi A H, Bryant H C, Harris P G et al. Phys. Rev. A, 1991, **43**: 1345-1365
- 11 Saha P K, hatakeyama S, Yamamoto K et al. Phys. Rev. ST Accel. Beams, 2011, **14**: 072801
- 12 Drozhdin A I, Rakhno I L, Striganov S I et al. Phys. Rev. ST Accel. Beams, 2012, **15**: 011002
- 13 Gulley M S, Keating P B, Bryant H C et al. Phys. Rev. A, 1996, **53**: 3201-3210
- 14 Webber R C, Hojvat C, IEEE Trans. Nucl. Sci. NS-26, 1979. 4012-4014
- 15 Chou W, Kostin M, Tang Z, Nucl. Instrum. Methods. Phys. Res. A, 2008, **590**: 1-12
- 16 Akasaka N, Koiso H, Oide K, et al., Operation software for commissioning of KEKB linac programmed with SAD, Proceedings of APAC, 1998. 495-497